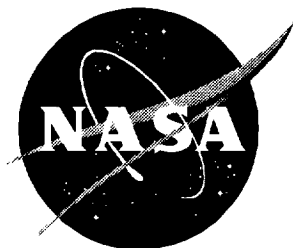# Problems Associated With Statistical Pattern Recognition of Acoustic Emission Signals in a Compact Tension Fatigue Specimen

Yolanda L. Hinton
U.S. Army Research Laboratory
Vehicle Technology Directorate
Langley Research Center, Hampton, Virginia

July 1999

Abstract

Acoustic emission (AE) data were acquired during fatigue testing of an aluminum 2024-T4 compact tension specimen using a commercially available AE system. AE signals from crack extension were identified and separated from noise spikes, signals that reflected from the specimen edges, and signals that saturated the instrumentation. A commercially available software package was used to train a statistical pattern recognition system to classify the signals. The software trained a network to recognize signals with a 91-percent accuracy when compared with the researcher's interpretation of the data. Reasons for the discrepancies are examined and it is postulated that additional preprocessing of the AE data to focus on the extensional wave mode and eliminate other effects before training the pattern recognition system will result in increased accuracy.

Introduction

Acoustic emission (AE) is defined as "the class of phenomena whereby transient elastic waves are generated by the rapid release of energy from localized sources within a material (or structure) or the transient waves so generated" (ref. 1). Acoustic emission can be generated by a variety of sources, including crack nucleation and propagation, multiple dislocation slip, twinning, grain boundary sliding, Barkhausen effect (realignment or growth of magnetic domains), phase transformations, and debonding and fracture of inclusion. Acoustic emission can also be generated by sources other than materials under stress, such as components rubbing against one another (fretting), leaks, structural vibrations, electrical transients. Spanner (ref. 2) and Williams (ref. 3) have provided discussions of sources of acoustic emission in a variety of materials and applications. Effective use of acoustic emission for monitoring damage progression in structures requires interpretation of the AE signals to determine the sources of the AE, their locations, and their severity. An experienced AE practitioner can learn to recognize signals from different sources, but always uncertainty about some of the data exists. Current AE systems, such as the one used in this study, can record up to 200 waveforms per second. Pattern recognition algorithms exist for training computers to recognize and interpret the signals. The objective of this project was to investigate the applicability of statistical pattern recognition to the identification of crack signals in a well-controlled test with limited sources of acoustic emission as a prelude to a possible application to monitoring crack growth in aging aircraft. The initial approach was to use a commercially available software package to extract features from the acoustic emission signals and perform the pattern recognition.

Pattern recognition methods require that a network first be trained to recognize signals; this is also called learning. A set of signals representing the different classes of data to be learned are provided as inputs to the network along with their classes. The network analyzes the differences between the signals and determines which characteristics best define each class of data. It compares its calculations with the known classes of the signals provided by the user. Where there is ambiguity, or disagreement with the classes provided, there is training error. The network can continue to refine its analysis to minimize the training error. Once the training error is minimized, the learning is complete and one or more classifiers are developed. These classifiers may be developed with the same technique used in the learning phase, or different techniques may be used.

The second phase of pattern recognition is classification. New signals are input to the network and analyzed by using the classifiers developed in the learning stage. The network does not know the classes of these signals but determines their classes based upon the classifiers. If several classifiers are used, they may not all agree on the classes of all the signals. If the user knows the classes of the signals, he may evaluate the results of the classification based upon his knowledge of the signals. Any discrepancies between the classifiers and the user's knowledge are classification errors.

In this work, a k-nearest neighbor algorithm was used in the learning phase, and the training error was

calculated and minimized. Classifiers were developed for the data by using k-nearest neighbor, Gaussian probability density, and Fisher linear discriminant methods. A detailed description of statistical pattern recognition and these classifiers is found in appendix A.

TestPro software by Infometrics, Inc., was used to perform the pattern recognition analysis. The software is part of a computer-based instrument for ultrasonic and eddy-current inspection and was developed specifically for those applications. The feature extraction module is particularly tailored to the analysis of these signals and not to acoustic emission signals. The statistical pattern recognition methods used, however, are generic and applicable to many problems in signal classification. Hinton (ref. 4) previously used this software to classify and recognize acousto-ultrasonic signals from defects in composite panels. In this composite panel study, five sets of panels, each with different model defects of varying severity, were examined and the data classified with TestPro software, with zero training error for four sets and 2 percent training error for the fifth set. The software was used in this study to determine its applicability to the classification of acoustic emission signals. The software is described in appendix B.

Experimental Procedure

A 2024-T4 aluminum compact tension specimen was tested in tension-tension fatigue. The specimen was a variation of that specified in reference 5. The specimen was approximately 21.24 cm (6 in.) square and 0.32 cm (1/8 in.) thick, with a straight-through notch of 6.35 cm (2.5 in.). The notch introduces a stress concentration that initiates crack growth under cyclic loading. The initial maximum and minimum loads were 3314 and 823 N (745 and 185 lb), respectively (load ratio R = 0.248). Four Digital Wave B1025 AE sensors were mounted on the specimen, as shown in figure 1, with silicone grease couplant and held on with C-clamps. These sensors have an amplitude response of ±15 dB and a phase response of $\pm3°$ in the range from 0.1 to 1 MHz, as shown in figure 2. The sensor output was amplified 40 dB by Digital Wave PA2040 G/A preamplifiers, then digitized and stored with a Digital Wave F4000 FWD AE analysis system. The AE system includes high and low pass filters and amplifiers on each channel, one of

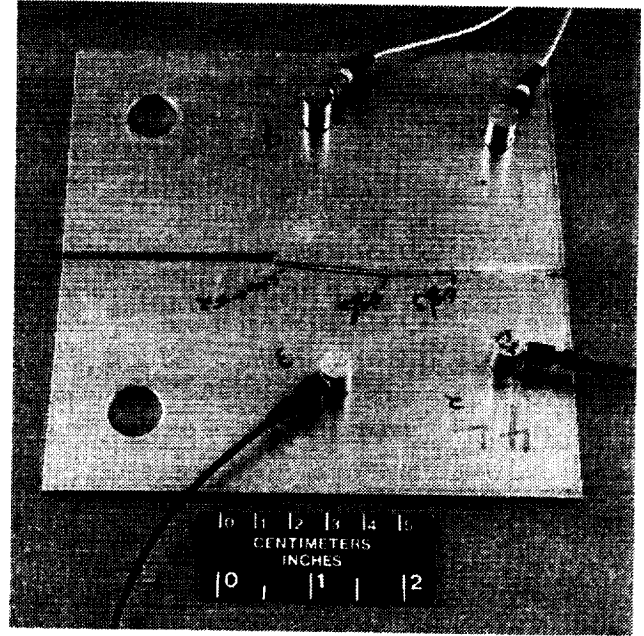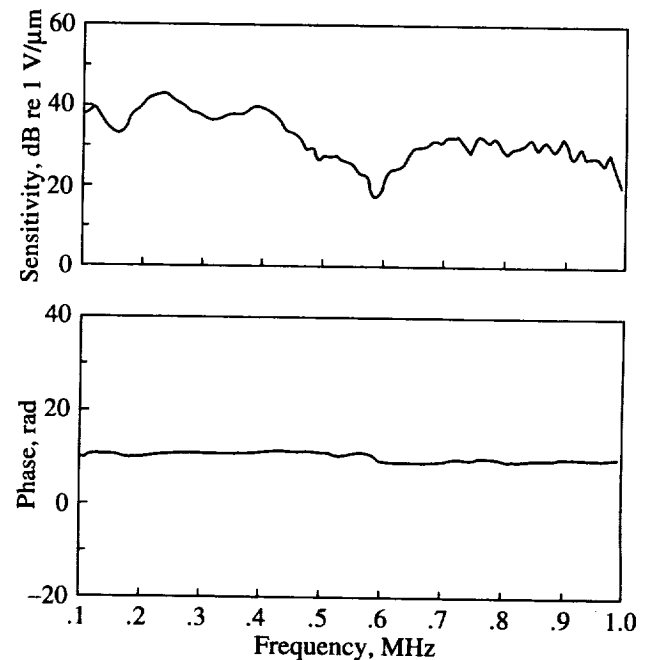Figure 1. 2024-T4 aluminum fatigue specimen with four acoustic emission sensors.

Figure 2. Absolute calibration of sensor, sensitivity, and phase, using laser interferometer to measure surface displacement, traceable to National Institute of Standards and Technology.

each for triggering and one of each for the data. The data channels were set to 0.02 MHz high pass and 1.5 MHz low pass filters and 30 dB gain. The trigger

2

circuitry was set to 0.3 MHz high pass and 1.0 MHz low pass filter, 36 dB gain, and 0.1-V threshold. The system triggers when the signal on any channel exceeds the threshold and then records data on all four channels. The system recorded 2048 points per waveform at 30 MHz sampling rate (0.033 μsec/point) with 25 percent pretrigger (512 points, 17.067 μsec pretrigger; 1536 points, 51.2 μsec posttrigger). The specimen was cycled at 1 Hz until a crack was visible to the naked eye. At that point the AE data acquisition began. A load gate was used during part of the test to allow the system to acquire AE data only during the highest 20 percent of the load, which is when crack extension is expected to occur. This reduces the amount of data from other sources such as crack face rubbing, which cannot occur when the crack opening load is exceeded. Figure 3 is a schematic of the test setup that shows the fatigue specimen with four sensors and preamplifiers and acoustic emission data acquisition system.
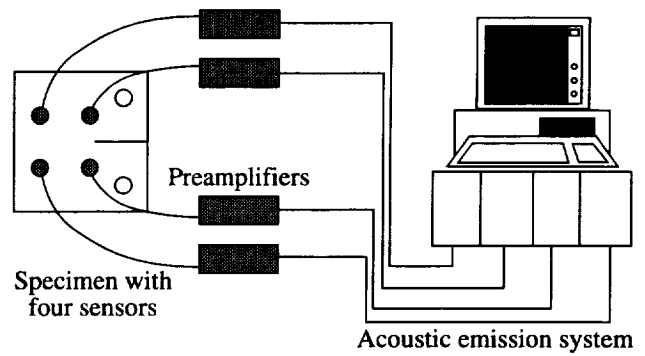

Figure 3. Schematic of test setup.

Analysis and Discussion

Two classes of signals were initially identified for training: cracks and noise. A typical crack signal is shown in figure 4 as received at all four sensors mounted on surface of fatigue specimen used during
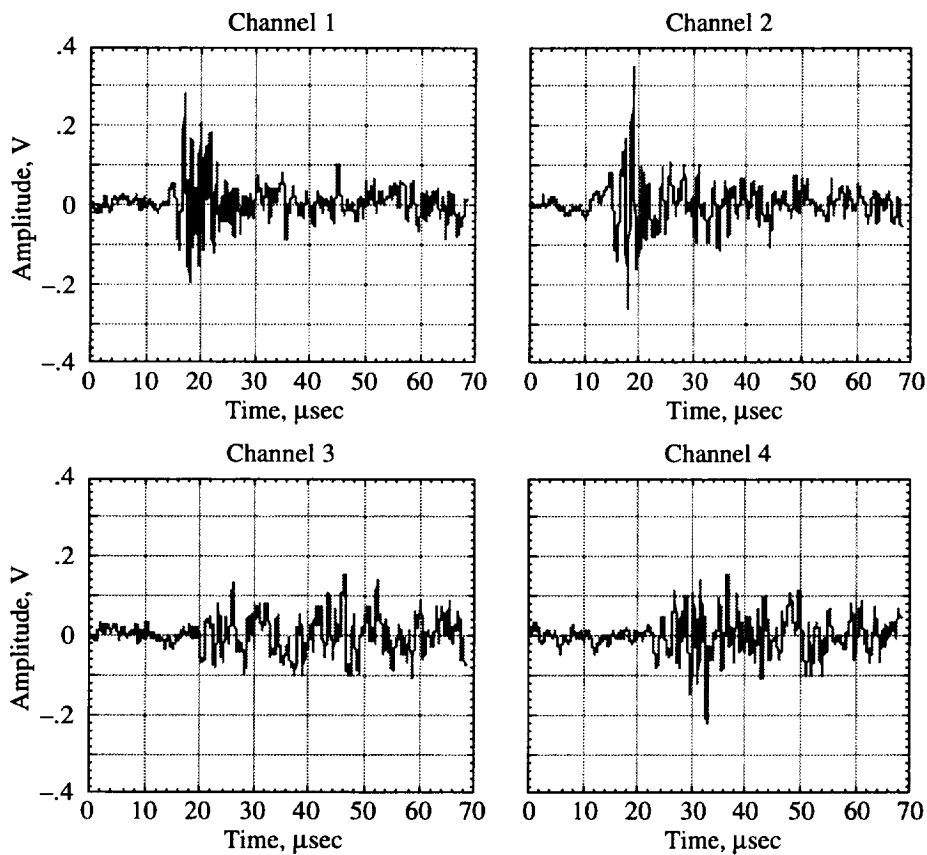

Figure 4. Typical crack signal as received at each of four sensors mounted on surface of fatigue specimen.

3

the test. The first 17 μsec of each signal is prior to the system being triggered. In this example, the signal first exceeds the 0.1-V threshold on channel 2. Channels 1 and 2 both show a rise time to peak amplitude within the next 2 to 3 μsec, and a decaying amplitude thereafter. The first one or two cycles of these signals are of lower frequency, followed by some higher frequency arrivals, an artifact of the extensional S_0 mode dispersion curves that have the very high frequencies traveling at a lower velocity than the earlier nondispersive low frequency modes. This signal appears to be a pure extensional mode wave with no flexural modes present, as expected for a through-thickness fatigue crack source, as discussed by Gorman (ref. 6). Signals resembling those shown in figure 4 were classified as crack signals; all others were grouped into the class of noise signals. Forty signals representative of cracks and 64 signals representative of noise signals were used to train a 6-nearest neighbor system. These signals were acquired with maximum and minimum loads of 2478 and 1757 N (557 and 395 lb). The software reported a training error of 0 percent. Fisher, Gaussian, and 3-nearest neighbor classifiers were developed, with reported classification errors of 6.7, 1.9, and 0 percent in classifying the training data. An additional 752 signals, acquired with load cycling from 3314 to 823 N (745 to 185 lb) and without the load gate, were then analyzed by each of the classifiers. Of these 752 signals, 276 showed characteristics of crack signals. The Fisher classifier reported 420 crack signals, the Gaussian classifier reported 604 crack signals, and the 3-nearest neighbor classifier reported 620 crack signals representing classification errors of at least 19 to 45 percent. Based on statistical pattern recognition concepts (ref. 7), these large discrepancies clearly indicate that the training set was not a good representation of the remaining data. Because these data were acquired without the use of a load gate, additional signals were likely acquired from other sources, for example, crack face rubbing and pin noise, that were not included in the training data. The class of noise signals was, therefore, redefined to accommodate some of these other sources.

After examining the 752 signals used for analysis, four classes of signals were identified: cracks, reflections, saturation, and spikes. Examples of these signals are shown in figure 5. The signals classified as reflections have significant oscillations during the pretrigger period. This type of signal is indicative of one that was reflected from the specimen edges and triggered the AE system to acquire new data as though from a separate signal. The saturation class comprises signals that saturated the electronics and were clipped. The spikes were very sharp, very short duration signals, typically of 1 to 2 μsec, which were believed to come from electrical noise. Training sets of 40 crack, 44 reflection, 40 saturation, and 20 spike signals were used to train the pattern recognition system. The minimum training error achieved for the 4-nearest neighbor algorithm was 9.5 percent. The Gaussian, Fisher, 3-, 4-, and 5-nearest neighbor classifiers were developed to analyze the additional data. The analysis resulted in classification errors of 5, 18, 10, 15, and 10 percent, which shows a significant increase in classification error over the case of two classes, cracks and noise. However, only one of the 40 training signals from cracks was improperly classified.

To evaluate the accuracy of the discriminant functions derived by the software, 564 signals, representing 141 events on each of 4 channels, were then analyzed by using each of the classifiers, and the results were compared with a personal evaluation of the unknown signals. The single Gaussian classifier resulted in the lowest classification error, with 8 of 59 (14 percent) crack signals wrongly identified as belonging to one of the other classes, and 8 of 91 (9 percent) signals which belong to other classes wrongly identified as cracks. The remaining signals did not appear to belong to any of the defined classes based on the characteristics described previously; therefore, they were not included in the analysis. Although the training errors using four classes are much higher than those using two classes, the actual classification of the additional waveforms showed improvement from errors in the 19- to 45-percent range with two classes, to about 10 percent in this case (16 of 150 signals). This error was, however, judged still to be unacceptably high, based on prior experience with this software (ref. 4). Therefore, an effort was made to further refine the definitions of the training sets. Because only one crack signal in the training set was wrongly classified, the noise signals were examined in an attempt to improve their representation in the training set.

Upon reexamination of the data, a fifth class of signals was identified. These signals are lower in frequency than the crack signals, suggesting an
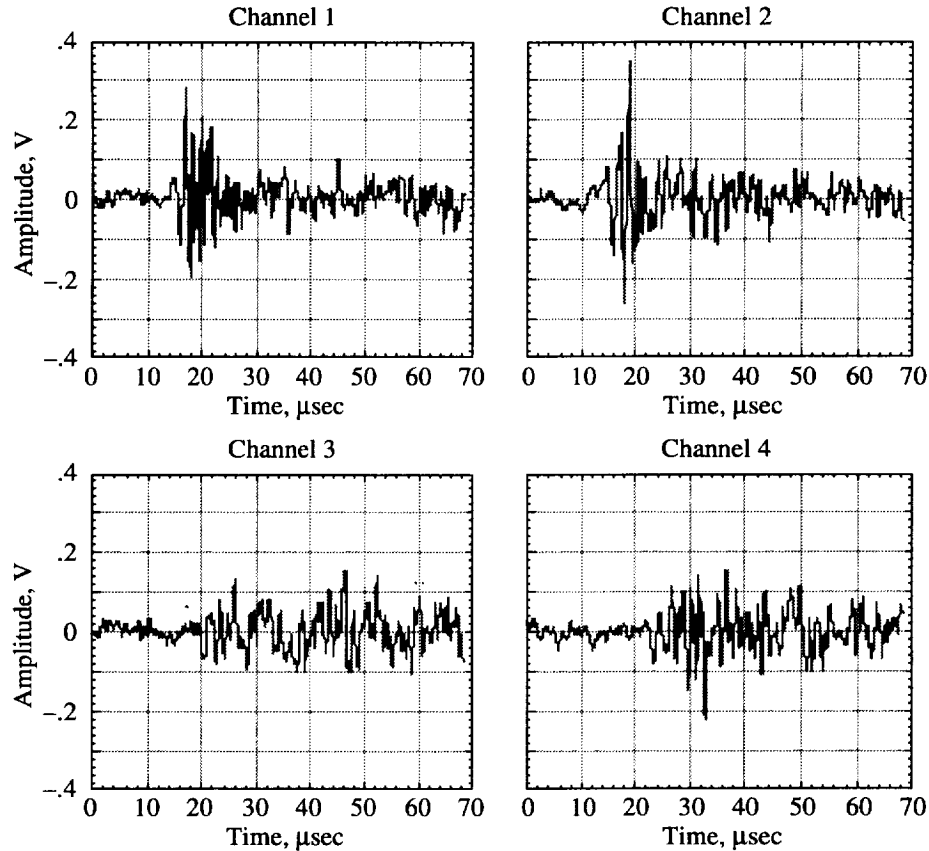
4

Figure 5. Representative signals from each of four classes: cracks, reflections, saturation, and spikes.

out-of-plane source motion or flexural wave, as discussed by Gorman and Prosser (ref. 8). They appear to occur at lower loads and may be indicative of crack face rubbing or pin loading noises. This fifth class was added to the training set, and the system trained again using the 4-nearest neighbor algorithm. The training error rose from 9 to 15 percent. The classification errors in identifying crack signals rose from 1 of 40 to 5 of 40; the remaining errors were in the other four classes.

Peak amplitude and peak-to-peak amplitude of acoustic emission signals are not effective means of identifying sources because signal amplitudes are greatly affected by attenuation. In figure 4, for example, the amplitude of the signals changes significantly for sensors at different distances from the crack, where propagation distances are only a few centimeters at most. Attenuation is even more significant when geometric spreading is dominant, when the wave modes are highly dispersive (as is the case with flexural waves), and in highly attenuating materials such as composites. Nevertheless, the decision was made to

add the amplitude features to the training set to determine if they would help further identify signals from each of the classes. The training process was then repeated for four and five training data sets. For four classes of data, the reduction in training error, from 9 to 7 percent, was insignificant; with five classes of data, these amplitudes had no effect on the training error.

According to Fukunaga (ref. 7), the training error and classification errors could indicate one or more of several problems:

1. The training set is not representative of the analysis data

2. The training set is too small, not indicative of the range of differences among the analysis signals

3. The features calculated by the software are not appropriate for analyzing these data

5

Inspection of the data indicates a fourth possible source of error: there are too many data points per signal; that is, there is too much extraneous information in the data. Each of these problems is discussed. Other effects, including mode conversion filtration and distortion of the original stress wave resulting from crack growth, the frequency response of the measurement system being too low to capture this wave, and edge reflection interferences, are also possible factors in the inability to use these methods.

The signals in the analysis data were chosen because they have the same visual characteristics as those in the training set. However, the statistical characteristics of the feature set are used for training and analysis. Poor agreement between training and analysis results indicates that the signals are statistically different.

Training the pattern recognition system requires a data set of sufficient size to analyze statistical differences in the data. The software recommends training sets of 10 or more signals. The training sets used were larger than this and should be of sufficient size. However, the signals used resulted from one acoustic emission event being detected at each of four sensors, and the signals change as they propagate along the plate. This results in signals that can have different visual, temporal, and statistical characteristics at each of the four sensors being included in the same class. Therefore, the training signals are possibly not truly representative of the variances in signals within each signal classification. This effect can be eliminated by using data only from the sensor at which the signal from each event was received first and only the first few microseconds of the recorded waveform.

The feature set was provided by the chosen software. It has been used successfully to characterize ultrasonic signals, which have some characteristics in common with acoustic emission signals. However, there are significant differences that may render these features inappropriate for this application. Further statistical analysis of the data may reveal other features that better identify the statistical differences in the signals.

Each crack event during the test causes signals to be recorded on each of four channels. All four channels begin recording when one channel is triggered, and some pretrigger data are also stored with the signal. Because the sensors are at different distances from the crack, the data on each channel include a varying amount of signal acquired before the crack signal reaches the sensor. The latter portions also show the effects of attenuation and dispersion before reception at the sensor. Gorman and Prosser (ref. 8) have shown that, for in-plane sources such as crack extension, the modal information indicative of extensional waves is in the first several microseconds of the signal. The latter part of the signal is dominated by reflections. The velocity of the extensional wave mode in 2024-T4 aluminum is 5380 m/sec. If the crack is 7.5 cm from the edge of the specimen, reflections of the original signal will return to the crack position within about 28 μsec. They would reach a transducer between the crack and the edge of the specimen even earlier. Thus, most of the information in the signals after the first 10 μsec or so is heavily affected by reflections and artifacts of geometry. Eliminating the pretrigger portion of the signal, and all but the first 10 μsec of the remaining signal, should focus on the extensional wave and eliminate much of the variation caused by reflections. Any attempt to using pattern recognition to classify acoustic emission signals as to their source must take into account that the signals are heavily affected by material properties and geometry. The other effects mentioned require additional experimentation to determine their relevance to the classification of these signals.

Concluding Remarks

In a laboratory fatigue test, TestPro software was unable to learn to classify acoustic emission signals from cracks with less than 9 percent classification error. This classification error may be acceptable in applications where multiple cracks, or very long cracks, can be tolerated. In applications where detection of small cracks, or small numbers of cracks, is critical, this classification error level is likely to be unacceptable. Further, where additional acoustic emission signals are generated from other sources, the classifiers developed may not be adequate to identify the signals from cracks. Further preprocessing of the acoustic emission signals may allow the software to classify the signals with greater accuracy. A different set of features that more accurately represents the differences observed in the signals may also give better accuracy.

6

Appendix A

Statistical Pattern Recognition

Pattern recognition approaches can be classified as either syntactic or statistical. With syntactic methods, the observations or signals to be analyzed are broken down into smaller parts, the way a language or sentence is parsed. The relationships between the parts are analyzed in a way similar to the ways that syntax rules express the relationships between parts of speech. These methods are used when a pattern is so complex that it is best analyzed as a composition of simpler subpatterns, as in fingerprint or scene analysis (ref. 9). Statistical methods, however, rely on mathematical models of the observations to be analyzed and the relationships among them. A set of measurements, or features, is extracted from each observation. These features should be invariant, or less sensitive to commonly encountered variations and distortions, and less redundant, than the observations themselves. These methods have been applied to waveform classification as summarized by Fukunaga (ref. 7) upon which the following discussion is based.

Statistical pattern recognition consists of, first, representing each observation as a vector in n-dimensional space, where each dimension n is a feature used to characterize each observation. Several such observations, represented by their vectors, form a distribution in feature space. Each distribution can be approximated by some probability density function, which expresses the likelihood that a vector which lies within the contour of the function belongs to that distribution. The boundaries which separate these distributions must be determined and expressed as mathematical functions, which are known as discriminant functions. Once these discriminant functions are determined, a pattern recognition network, or classifier, analyzes a given vector and determines to which distribution it belongs. The process of finding the proper discriminant function is called learning or training; the samples used to design the classifier comprise the training set.

For simplicity in discussing classifier design, consider the case of two distributions or classes. Ideally these two classes are totally distinct and separate in feature space with no overlap. In this case, the training

error is zero, and designing a classifier requires only consideration of the region in feature space between the classes. One can develop a linear classifier by drawing a line bisecting and perpendicular to a line connecting the means of the two classes. This process gives a simple method for classifying observations that fall on either side of the line. Observations that fall directly on the line can be classified randomly or rejected.

In the more general case, the classes are not totally distinct and separate in feature space, but do overlap; this results in training error. The classifier must be designed to minimize the error associated with observations in the overlap region. Let X be a random n-dimensional vector, as discussed in Papoulis (ref. 10), whose components are features representing a test sample, that is, an observation to be classified. In figure A1, ω_1 and ω_2 are two classes in feature space. We define a linear discriminant function $h(x)$ as:

$$h(x) = V^T X + v_0 \underset{\omega_2}{\overset{\omega_1}{\gtrless}} 0 \qquad (1)$$

The vector X is projected onto a vector V, whose transpose is V^T, and the variable $y = V^T X$ in the projected one-dimensional h-space is classified to either ω_1 or ω_2 depending on whether $h(x) < 0$ or $h(x) > 0$. Figure A1 shows two possible choices of V and the
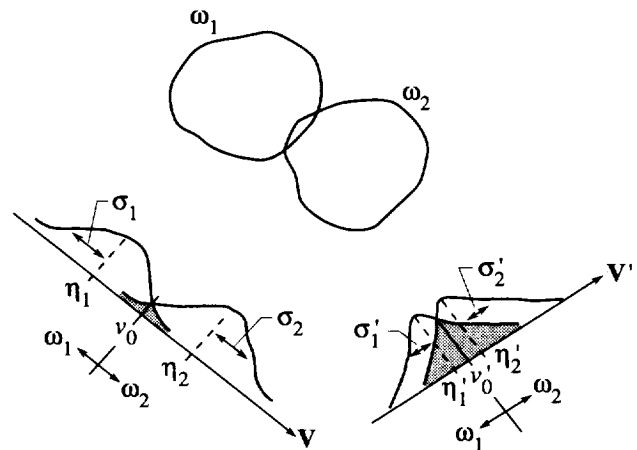

Figure A1. Example of linear mapping, showing two classes, ω_1 and ω_2, mapped onto vectors V and V' with errors v_0 and v_0'. (From ref. 7 (used with permission).)

corresponding choices of v_0. The optimum classifier selects the values of V and v_0 which give the smallest error in the projected h-space. The Fisher criterion f for determining the optimum V and v_0 is

$$f = \frac{(\eta_1 - \eta_2)^2}{\sigma_1^2 + \sigma_2^2} \qquad (2)$$

where η_1, η_2, σ_1^2, and σ_2^2 are the means and variances, respectively, of the classes ω_1 and ω_2, and f measures the differences of the two means normalized by the average variance. The means η_i and variances σ_1^2 can be expressed in terms of V and v_0 as

$$\eta_i = V^T M_i + v_0 \qquad (3)$$

$$\sigma_i^2 = V^T \Sigma_i V \qquad (4)$$

where

Σ_i covariance matrix of ω_i

M_i expected vector or mean of X_i

Substituting equations (3) and (4) into equation (2), differentiating with respect to V and v_0, and setting the derivative equal to zero yield V with the minimum error as follows:

$$V_{min} = \left[\frac{1}{2}\Sigma_1 + \frac{1}{2}\Sigma_2\right]^{-1} (M_2 - M_1) \qquad (5)$$

Substituting equation (5) into equation (1) yields the Fisher linear discriminant function $h_F(x)$,

$$h_F(x) = \left\{\left[\frac{1}{2}\Sigma_1 + \frac{1}{2}\Sigma_2\right]^{-1} (M_2 - M_1)\right\}$$

$$\times (X + v_0) \underset{\omega_2}{\overset{\omega_1}{\gtrless}} 0 \qquad (6)$$

Linear discriminant functions are optimum only for normal distributions with equal covariance matrices. The assumption of equal covariance matrices is rea-

sonable in many applications involving signal detection where the noise is random and does not change from one signal to another.

The random vector X, with n variables $\begin{bmatrix} x_1 & x_2 & \dots & x_n \end{bmatrix}^T$, is the input to the pattern recognition network. It is a property of a random vector that it can be characterized by a probability distribution function $P(X)$;

$$P(x_1, \dots, x_n) = Pr(x_1 \le x_1, \dots x_n \le x_n) \qquad (7)$$

which may also be written

$$P(X) = Pr\{X \le X\} \qquad (8)$$

where $Pr\{A\}$ is the probability of an event A, and X is a given vector. It is also a property of a random vector that it can be characterized by a density function $p(X)$, the derivative of the distribution function,

$$pX = \lim_{\substack{\Delta x_1 \to 0 \\ \Delta x_n \to 0}} \frac{Pr\{x_1 < x_1 < x_1 + \Delta x_1, \dots, x_n < x_n \le x_n + \Delta x_n\}}{\Delta x_1 \dots \Delta x_n}$$

$$= \frac{\partial^n PX}{\partial x_1 \dots \partial x_1} \qquad (9)$$

denoting differentiation of the distribution function with respect to each of the components of the vector X. The density function $p(X)$ is not a probability, but must be multiplied by a region ΔX to obtain a probability. An explicit expression of $p(X)$ for a normal distribution is

$$N_x(M, \Sigma) = \frac{1}{(2\pi)^{n/2}|\Sigma|^{1/2}} \exp\left[-\frac{1}{2} d^2(X)\right] \qquad (10)$$

where $N_x(M,\Sigma)$ is a normal distribution with expected vector M and covariance matrix Σ, and

$$d^2(X) = \sum_{i=1}^{n} \sum_{j=1}^{n} h_{ij}(x_1 - m_i)(x_j - m_j) \qquad (11)$$

8

where h_{ij} is the i,j component of Σ^{-1}, the inverse covariance matrix, and m_i is the expected value or mean of x_i. The coefficient $(2\pi)^{-n/2}|\Sigma|^{-1/2}$ is selected to satisfy the probability condition

$$\int p(X)\, dX = 1 \qquad (12)$$

Equation (10) expresses the probability that a given vector X is a member of the class defined by the normal distribution N. The Gaussian probability density function classifier assigns the test sample to the class for which this function is maximum.

In the k-nearest neighbor approach, the k nearest neighbors (kNN's) of a test sample are selected from the mixture of classes in feature space, and the number of neighbors from each class among the k selected samples is counted. The test sample is then classified to the class represented by a majority of the kNN's. Ties can be broken at random or rejected and not classified (ref. 11).

Appendix B

TestPro Software

TestPro software by Infometrics, Inc., is a computer-based instrument for ultrasonic and eddy-current inspection. The software incorporates data acquisition and analysis routines into a package specifically tailored for these applications. The feature extraction and pattern recognition modules use standard statistical algorithms; however, the selection of features to extract from the signals is specifically chosen to be applicable to ultrasonic and eddy-current signals commonly encountered in nondestructive evaluation. Acoustic emission signals bear some similarity to ultrasonic signals, particularly when ultrasonic sensors are used for their detection. They are very different, however, in that they are generated by physical and mechanical phenomena in a material or structure, whereas ultrasonic signals are applied to a structure which then interacts with and modifies the signals. Although the TestPro software was developed specifically for ultrasonic and eddy-current analysis, it was used here to determine its applicability to the study of acoustic emission signals.

Feature Extraction

TestPro software preprocesses each waveform, then calculates 71 features, 35 from the time domain signal and 36 from the frequency domain, as listed in table B1. Preprocessing consists of subtracting the mean value of the waveform data from each point. This process minimizes the direct-current (dc) component in the frequency domain resulting from the fast Fourier transform (FFT), but this does not necessarily result in the endpoints of the signal being zero. Since nonzero endpoints can cause spurious high frequency components to appear in the power spectrum, it is desirable to force the endpoints to zero. This forcing is accomplished by multiplying the first and last eight points of the signal by a cosine function. The number of data points is increased to the next power of 2 and padded with zeros to perform the FFT.

The time domain features are extracted from the waveform, the cumulative distribution of the waveform, and the envelope of the waveform. The waveform features are maximum absolute value of the amplitude, or peak amplitude, and maximum peak-to-peak amplitude. The waveform is then normalized by dividing all amplitude values by the peak amplitude, resulting in an amplitude range from -0.1 to 0.1. Because the mean value of the waveform was subtracted, the resulting mean is 0; the standard deviation of the normalized amplitude values is calculated and stored as a waveform feature.

The cumulative distribution of the normalized signal is calculated by computing a running sum of squares of the signal amplitude versus time. The final value of the running sum is equal to the total power of the signal. The cumulative distribution is analyzed to determine the points in time where the distribution crosses 25, 50, 75, and 90 percent of the total power. The differences between the 50- and 25-percent levels, the 75- and 25-percent levels, and the 90- and 25-percent levels are added to the feature set.

The envelope of the signal is determined by applying a smoothing function to the positive amplitude peaks of the signal. It approximates a numeric integration of the waveform. The resulting envelope is normalized by dividing by the peak amplitude, and the mean and standard deviation are computed and included in the feature set. The remaining time domain features are measured from rise and fall time characteristics of the envelope. Rise and fall times are determined at points where the envelope crosses thresholds of 25, 50, and 75 percent of the peak amplitude. Local rise and fall times are those times at which the threshold crossing is nearest the maximum value of the envelope; global rise and fall times are those at which the threshold crossing is farthest from the peak. Rise and fall slopes indicate how fast the envelope function rises or falls; rise and fall variances indicate the variation of amplitude values between the thresholds and the peak. To calculate the slopes and variances, TestPro software performs a linear least-squares regression on the data points between each threshold crossing and the peak amplitude. Global and local pulse durations are calculated by subtracting the corresponding rise and fall times.

The frequency domain features are measured from the power spectrum of the normalized waveform and the cumulative distribution of the power spectrum. The FFT is calculated and the squares of the real and imaginary components are summed to generate a power spectrum, which is then normalized by the power level. The mean and standard deviation of the normalized power spectrum are calculated and included in the feature set.

10

The frequency at which the maximum values of the power spectrum occurs is located. The local 50-percent rise and fall frequencies are the half-power points closest to the frequency of the peak power. The center frequency is defined as the average of the local 50-percent rise and fall frequencies. The bandwidth is the difference of these two frequencies divided by the frequency of the peak and expressed as a percentage. Local and global spectral features are determined in a manner similar to the local and global time domain features described earlier. Fractions of total power estimates are measured by computing the power contributions over the relevant frequency intervals as specified in table B1 (features 44–47), then dividing by the power contribution between the local rise and fall frequencies at 25 percent of the peak power. The remaining frequency domain features are analogous to those measured from the envelope function in the time domain.

Feature Selection

TestPro software uses a k-nearest neighbor algorithm to analyze the waveform features and to learn to distinguish signals from different classes. This learning requires a set of known signals for each of the classes. The value of k used for learning is the square root of the number of signals in the smallest set of the training data.

TestPro software first attempts to classify the signals using each feature individually. For each waveform in the database, its k nearest neighbors are identified by using minimum distance in a single dimension. Using the class value of the majority of the k nearest neighbors, a class call for the waveform is determined. If this class call is not the same as the given class of the waveform, an error counter is incremented. This process is repeated for all waveforms in the training set for the single feature being analyzed; this results in an estimate of the classification error using the single feature. This process is repeated to obtain a single error estimate for each feature. The feature with the minimum single error is selected as the optimum feature. The entire process is repeated to determine the second optimum feature. The nearest neighbor criterion now involves computation of a two-dimensional distance to determine the k nearest neighbors, where the first dimension is the first optimum feature and the second is the feature being analyzed. The error analysis is again performed for each feature,

and the feature with the minimum error is added to the set of optimum features. This process is repeated, with the distance determination expanding to multiple dimensions until either the number of optimum features equals 10, adding another feature to the optimum set results in no further reduction of the overall error is achieved.

TestPro software then allows several classifiers or discriminants to be developed to be used for analyzing unknown signals. These are the Gaussian probability density function, a Fisher linear discriminant, and k-nearest neighbor nonlinear discriminant function, where k ranges from 1 to 20.

Waveform Analysis

Waveform analysis is the process of classifying unknown signals. Each classifier, or discriminant function, is used to determine the probability of each unknown waveform belonging to each of the classes defined in the learning process. The total probability sums to 100 percent over all the classes for each waveform.

Each classifier uses some measure of the distance between the feature values of the waveform being analyzed and the mean values of the features used in training to determine the class probabilities. A confidence level is also given as an indication of how closely the evaluation point fits the mean values of the training data. Each feature is scaled by subtracting the mean value of the training set and dividing by its standard deviation. This value represents the distance between the feature being evaluated and the mean of the training set in standard deviations. This distance is determined for each of the defined classes and converted to a qualitative confidence level. If the difference is less than or equal to two standard deviations (2σ), the confidence level is high. A difference greater than 2σ and less than or equal to 3σ is a medium confidence level. A difference greater than 3σ is a low confidence level. The confidence level of the minimum difference is assigned to the feature being evaluated.

This process is repeated for each additional feature in the optimum feature set. An overall confidence level is determined by selecting the maximum of the sealed differences for each feature and converting it to a confidence level.

Table B1. Waveform Features Calculated by TestPro Software

Feature	Description
Radio frequency (RF) waveform	
1	Maximum absolute amplitude of RF waveform
2	Maximum peak-to-peak amplitude of RF waveform
3	Mean value of normalized RF waveform amplitude values
4	Variance of normalized RF waveform amplitude values
RF waveform cumulative distribution (CD)	
5	Difference between 50- and 25-percent level (RF waveform CD)
6	Difference between 75- and 25-percent level (RF waveform CD)
7	Difference between 90- and 25-percent level (RF waveform CD)
RF waveform envelope function	
8	Local pulse duration between 25-percent levels
9	Global pulse duration between 25-percent levels
10	Mean value of normalized envelope function
11	Variance of normalized envelope function
12	Local rise time from 25-percent level to peak
13	Local rise time from 50-percent level to peak
14	Local fall time from peak to 25-percent level
15	Local fall time from peak to 50-percent level
16	Local rise slope between 25-percent level and peak
17	Local rise variance between 25-percent level and peak
18	Local rise slope between 50-percent level and peak
19	Local rise variance between 50-percent level and peak
20	Local fall slope between peak and 25-percent level
21	Local fall variance between peak and 25-percent level
22	Local fall slope between peak and 50-percent level
23	Local fall variance between peak and 50-percent level
24	Global rise time from 25-percent level to peak
25	Global rise time from 50-percent level to peak
26	Global fall time from peak to 25-percent level
27	Global fall time from peak to 50-percent level
28	Global rise slope between 25-percent level and peak
29	Global rise variance between 25-percent level and peak
30	Global rise slope between 50-percent level and peak
31	Global rise variance between 50-percent level and peak
32	Global fall slope between peak and 25-percent level
33	Global fall variance between peak and 25-percent level
34	Global fall slope between peak and 50-percent level
35	Global fall variance between peak and 50-percent level
Spectrum cumulative distribution	
36	Difference between 25- and 50-percent level (spectrum CD)
37	Difference between 25- and 75-percent level (spectrum CD)
38	Difference between 25- and 90-percent level (spectrum CD)

12

Table B1. Concluded

Feature	Description
	Power spectrum
39	Frequency of maximum value of power spectrum
40	Center frequency of power spectrum
41	Measured bandwidth
42	Mean value of normalized power spectrum
43	Variance of normalized power spectrum
44	Fraction of total power between lower 25-percent level and peak
45	Fraction of total power between lower 50-percent level and peak
46	Fraction of total power between peak and upper 25-percent level
47	Fraction of total power between peak and upper 50-percent level
48	Local rise frequency from 25-percent level to peak
49	Local rise frequency from 50-percent level to peak
50	Local fall frequency from peak to 25-percent level
51	Local fall frequency from peak to 50-percent level
52	Local rise slope between 25-percent level and peak of spectrum
53	Local rise variance between 25-percent level and peak of spectrum
54	Local rise slope between 50-percent level and peak of spectrum
55	Local rise variance between 50-percent level and peak of spectrum
56	Local fall slope between peak of spectrum and 25-percent level
57	Local fall variance between peak of spectrum and 25-percent level
58	Local fall slope between peak of spectrum and 50-percent level
59	Local fall variance between peak of spectrum and 50-percent level
60	Global rise frequency between 25-percent level and peak of spectrum
61	Global rise frequency between 50-percent level and peak of spectrum
62	Global fall frequency between peak of spectrum and 25-percent level
63	Global fall frequency between peak of spectrum and 50-percent level
64	Global rise slope between 25-percent level and peak of spectrum
65	Global rise variance between 25-percent level and peak of spectrum
66	Global rise slope between 50-percent level and peak of spectrum
67	Global rise variance between 50-percent level and peak of spectrum
68	Global fall slope between peak of spectrum and 25-percent level
69	Global fall variance between peak of spectrum and 25-percent level
70	Global fall slope between peak of spectrum and 50-percent level
71	Global fall variance between peak of spectrum and 50-percent level

References

1. Standard Terminology for Nondestructive Examinations. E 1316-96, *Nondestructive Testing, Annual Book of ASTM Standards,* Volume 03.03, 1996, pp. 609–644.

2. Spanner, Jack C.: *Acoustic Emission—Techniques and Applications.* Intex Publ. Co., 1974.

3. Williams, R. V.: *Acoustic Emission.* A. Hilger, 1980.

4. Hinton, Yolanda L.: Application of Pattern Recognition Techniques to Acousto-Ultrasonic Testing of Kevlar™ Composite Panels. *Second International Conference on Acoustic-Ultrasonics.* Alex Vary, ed., American Soc. Nondestruct. Testing, Inc., 1993, pp. 125–132.

5. Standard Test Method for Plane-Strain Fracture Toughness of Metallic Materials. E 399-90 (Reapproved 1997). *Metals—Mechanical Testing; Elevated and Low-Temperature Tests; Metallography, Annual Book of ASTM Standards,* Volume 03.01, 1997, pp. 408–438.

6. Gorman, Michael R.: Determining Fatigue Crack Growth in Aircraft by Monitoring Acoustic Emission. *Naval Res. Rev.,* vol. XLIV, 1992, pp. 24–27.

7. Fukunaga, Keinosuke: *Introduction to Statistical Pattern Recognition,* Second ed., Academic Press, 1990.

8. Gorman, Michael R.; and Prosser, William H.: AE Source Orientation by Plate Wave Analysis. *J. Acoust. Emiss.,* vol. 9, no. 4, 1990, pp. 283–288.

9. Fu, K. S., ed.: *Digital Pattern Recognition,* Second corr. & updated ed., Springer-Verlag, 1980.

10. Papoulis, Athanasios: *Probability, Random Variables, and Stochastic Processes,* Second ed., McGraw-Hill, 1984.

11. Devijver, Pierre A.; and Kittler, Josef: *Pattern Recognition—A Statistical Approach.* Prentice Hall Int., 1982.

REPORT DOCUMENTATION PAGE

Public reporting burden for this collection of information is estimated to average 1 hour per response, including the time for reviewing instructions, searching existing data sources, gathering and maintaining the data needed, and completing and reviewing the collection of information. Send comments regarding this burden estimate or any other aspect of this collection of information, including suggestions for reducing this burden, to Washington Headquarters Services, Directorate for Information Operations and Reports, 1215 Jefferson Davis Highway, Suite 1204, Arlington, VA 22202-4302, and to the Office of Management and Budget, Paperwork Reduction Project (0704-0188), Washington, DC 20503.

1. AGENCY USE ONLY *(Leave blank)*	2. REPORT DATE July 1999	3. REPORT TYPE AND DATES COVERED Technical Publication	

4. TITLE AND SUBTITLE
Problems Associated With Statistical Pattern Recognition of Acoustic Emission Signals in a Compact Tension Fatigue Specimen

5. FUNDING NUMBERS
WU 538-10-11-03
PR A5008

6. AUTHOR(S)
Yolanda L. Hinton

7. PERFORMING ORGANIZATION NAME(S) AND ADDRESS(ES)
U.S. Army Research Laboratory
Vehicle Technology Directorate
NASA Langley Research Center
Hampton, VA 23681-2199

8. PERFORMING ORGANIZATION REPORT NUMBER
L-17740

9. SPONSORING/MONITORING AGENCY NAME(S) AND ADDRESS(ES)
National Aeronautics and Space Administration
Washington, DC 20546-0001
and
U.S. Army Research Laboratory
Adelphi, MD 20783-1145

10. SPONSORING/MONITORING AGENCY REPORT NUMBER
NASA/TP-1999-209351
ARL-TR-1691

11. SUPPLEMENTARY NOTES
Hinton: U.S. Army Research Laboratory, Vehicle Technology Directorate, Langley Research Center, Hampton, VA.

12a. DISTRIBUTION/AVAILABILITY STATEMENT

Unclassified–Unlimited
Subject Category 71   Distribution: Standard
Availability: NASA CASI (301) 621-0390

12b. DISTRIBUTION CODE

13. ABSTRACT *(Maximum 200 words)*

Acoustic emission (AE) data were acquired during fatigue testing of an aluminum 2024-T4 compact tension specimen using a commercially available AE system. AE signals from crack extension were identified and separated from noise spikes, signals that reflected from the specimen edges, and signals that saturated the instrumentation. A commercially available software package was used to train a statistical pattern recognition system to classify the signals. The software trained a network to recognize signals with a 91-percent accuracy when compared with the researcher's interpretation of the data. Reasons for the discrepancies are examined and it is postulated that additional preprocessing of the AE data to focus on the extensional wave mode and eliminate other effects before training the pattern recognition system will result in increased accuracy.

14. SUBJECT TERMS
Acoustic emission; Signal classification; Pattern recognition; Fatigue testing

15. NUMBER OF PAGES
19

16. PRICE CODE
A03

17. SECURITY CLASSIFICATION OF REPORT Unclassified	18. SECURITY CLASSIFICATION OF THIS PAGE Unclassified	19. SECURITY CLASSIFICATION OF ABSTRACT Unclassified	20. LIMITATION OF ABSTRACT UL

NSN 7540-01-280-5500